FINITE-ELEMENT ANALYSIS OF RIGID PAVEMENTS WITH PARTIAL SUBGRADE CONTACT

Y. H. Huang and S. T. Wang, University of Kentucky

A finite-element method programmed for a high-speed computer was developed for determining the stresses and deflections in concrete pavements with partial subgrade contact. The partial contact may result from the pumping and plastic deformation of the subgrade in combination with the upward warping of the slabs. The method is based on the classical theory of thin plates on Winkler foundations. The condition of contact is illustrated by spring analogies. If pumping and plastic deformation of the subgrade are negligible, the foundation is considered as a set of springs, the tops of which are all at the same elevation. If pumping and plastic deformation exist, the tops of the springs will be at different elevations, and that must be specified before an analysis can be made. The deformed shape of the slabs due to the combined effect of weight and warping is determined first and then used for computing the stresses and deflections due to wheel loads. The accuracy of the method for computing temperature stresses is verified by the assumption that the slab and the subgrade are in full contact and by making a comparison with Westergaard's exact solutions. The validity of the method in predicting the stresses and deflections in actual pavements is indicated by a comparison with the experimental measurements from the AASHO Road Test. The solutions based on partial contact check more closely with the experimental measurements than with those based on full contact.

•WHEN Westergaard (1) developed his theoretical method for computing the stresses in rigid pavements, he made 2 major assumptions. The first assumption is that the subgrade acts as a Winkler foundation consisting of a series of springs. The reactive pressure between the slab and the subgrade is directly proportional to the deflection with a constant of proportionality, which he called the modulus of subgrade reaction or k value. Although the k value is a fictitious quantity not characteristic of the subgrade only but depending also on other factors, the use of it greatly facilitates the analysis. Furthermore, the k value does not have a large effect on the stresses, and an approximate estimation will suffice for design purposes. The second assumption, which has been open to more skepticism, is that the slab and the subgrade are always in full contact. This assumption implies that the reactive pressure between the slab and the subgrade always exists no matter how the slab deflects. If the slab deflects upward at a certain point, the reactive pressure at that point will be downward, i.e., the subgrade will pull the slab down. This assumption is reasonable if each spring in the Winkler foundation functions perfectly and the weight of the slab imposes a uniform precompression on the spring. As long as the upward deflection is smaller than the precompression, the slab and the spring will be in contact. However, if some of the springs become defective because of pumping or plastic deformation, the assumption of full contact will no longer hold.

Publication of this paper sponsored by Committee on Rigid Pavement Design.

Although Westergaard's analysis based on full contact can predict the stresses due to interior loading quite satisfactorily, it has great difficulty in predicting the stresses due to corner loading because the corner areas are normally not in contact with the subgrade. Results from the Arlington test (2) indicated that the pavement and the subgrade were not in full contact even if the slab was flat and there was no temperature differential between the top and the bottom. It was also found that the stresses in concrete pavements due to corner loading depended strongly on the condition of warping. When the corner was warped down and the slab and subgrade were in full contact, the observed corner stresses checked favorably with Westergaard's solutions. However, the observed stresses were 40 to 50 percent greater when the corner was warped up. Consequently, Westergaard's equation for corner loading was modified by Bradbury (3), Kelley (4), Spangler (5), and Pickett (6) to account for the loss of subgrade contact due to temperature warping, pumping, and plastic deformation of the subgrade. These modifications were based on empirical results, and no theoretical methods to the authors' knowledge have been developed so far. With the advent of high-speed computers and the finite-element method, it is now possible to analyze concrete pavements subjected to warping and loading without assuming that the slab and the subgrade are in full contact. It is believed that the method presented here is original and should provide a useful tool for the design and analysis of rigid pavements.

In a previous paper (7), the authors developed a finite-element method for analyzing concrete slabs with load transfer at the joints. The effect of partial contact between the slab and the subgrade was evaluated by simply deleting the reactive forces at those nodes that were assumed not to be in contact. In view of the fact that a node not in contact before loading might become in contact after loading and vice versa, it was indicated that, if the condition of contact at various nodes was specified, the stresses and deflections in the slabs could be determined by the finite-element analysis in which a method of successive approximations was used. It is the purpose of this paper to present such a method for analyzing concrete pavements with partial subgrade contact.

In this paper, the concept of full contact is discussed first. A general method, applicable to both full and partial contact, is then presented for computing the stresses and deflections in the slabs due to temperature warping. The accuracy of the method is verified by the assumption that the slab and the subgrade are in full contact and by a comparison with Westergaard's exact solutions. Next, 2 cases of partial contact are discussed. In the first case, there is no pumping or plastic deformation of the subgrade, so the springs in the Winkler foundation are all of the same length. Partial contact is caused by the upward warping of the slabs and occurs only near the pavement edges or corners. In the second case, there is pumping or plastic deformation of the subgrade, so the springs are assumed to be of unequal lengths. Partial contact is caused by the unequal length of the springs and possibly by the upward warping of the slabs. Finally, the finite-element solutions are compared with the experimental measurements from the AASHO Road Test. The solutions based on partial contact check more favorably with the experimental measurements than those based on full contact, thus indicating the validity of the method.

ANALYSIS BASED ON FULL CONTACT

The finite-element analysis of concrete pavements based on full contact and subjected to wheel loads was presented in the previous paper (7) and will not be repeated here. Only the case involving temperature warping is presented here. Before the theoretical formulation is presented, it may be worthwhile to discuss the concept of full contact by the spring analogy shown in Figure 1. Figure 1a shows a Winkler foundation consisting of a series of springs, each representing a nodal point in the finite-element analysis. When a slab is placed on the foundation, the weight of the slab will cause a precompression of the springs, as shown in Figure 1b. Because the slab is uniform in thickness, each spring will deform the same amount, and no stresses will be induced in the slab. The amount of precompression can be determined directly by dividing the weight of slab per unit area by the modulus of subgrade reaction. When the temperature is colder at the top of the slab than that at the bottom, as is usually

the case at night, part of the slab will deflect upward, as shown in Figure 1c. However, the slab and the springs still remain in contact because the upward deflections are smaller than the precompression. The deflection of the slab due to warping can be determined by subtracting the precompression due to the weight of slab from the deflection due to the weight and the warping combined, as indicated by the shaded area in Figure 1c. The result is exactly the same as when the warping alone is considered. The same is true when a load is applied to a warped slab, as shown in Figure 1d. Therefore, when the slab and the subgrade are in full contact, the principle of superposition applies. The stresses and deflections due to warping and loading can be determined separately, one independent of the other, disregarding the weight of the slab. This principle forms the basis of Westergaard's analysis.

Stresses and Deflections Due to Warping

The general formulation involving warping is similar to that for loading, as described in the previous paper (7). After the stiffness matrix is superimposed over all elements and the nodal forces are replaced with the statistical equivalent of the externally applied loads, the following simultaneous equations can be obtained for solving the nodal displacements.

$$[K]\{\delta\} = \{F\} + k[A]\{\delta'\} \tag{1a}$$

where

- $[K]$ = stiffness matrix of the slab,
- $\{\delta\}$ = nodal displacements,
- $\{F\}$ = nodal forces due to applied loads,
- k = modulus of subgrade reaction,
- $[A]$ = diagonal matrix representing the area over which subgrade reaction is distributed, and
- $\{\delta'\}$ = subgrade displacements.

Note that the second term on the right side of Eq. 1a represents the nodal forces due to the subgrade reaction. If the slab has a total of n nodes, then

$$\{\delta\} = \begin{Bmatrix} \delta_1 \\ \vdots \\ \delta_i \\ \vdots \\ \delta_n \end{Bmatrix} \quad \{F\} = \begin{Bmatrix} F_1 \\ \vdots \\ F_i \\ \vdots \\ F_n \end{Bmatrix} \quad [A] = \begin{bmatrix} A_1 & \cdots & 0 & \cdots & 0 \\ \vdots & & \vdots & & \vdots \\ 0 & \cdots & A_i & \cdots & 0 \\ \vdots & & \vdots & & \vdots \\ 0 & \cdots & 0 & \cdots & A_n \end{bmatrix} \tag{1b}$$

and

$$\delta_i = \begin{Bmatrix} w_i \\ \theta_{xi} \\ \theta_{yi} \end{Bmatrix} \quad F_i = \begin{Bmatrix} F_{wi} \\ 0 \\ 0 \end{Bmatrix} \quad \delta_i' = \begin{Bmatrix} c_i - w_i \\ 0 \\ 0 \end{Bmatrix} \tag{1c}$$

where

- i = subscript indicating the ith node;
- w = vertical deflection, downward positive;
- θ_x = rotation about x axis;
- θ_y = rotation about y axis;
- F_w = vertical force due to externally applied load, downward positive; and
- c = initial curling of a weightless and unrestrained slab due to a temperature differential between the top and the bottom.

Note that c = 0 when there is no warping. The reason that F_i and δ'_i contain only one nonzero element is that the nodal forces are determined by statics and only vertical loads and reactions are involved.

Figure 2 shows, in an exaggerated scale, a thin slab subjected to a temperature differential, Δt, between the top and the bottom. If the slab is weightless and unrestrained, it will form a spherical surface with a radius R. Because the slab is only slightly curved, the length of the arc on the upper surface is practically the same as that on the lower surface, so the length L of the upper surface is shown as the length of the lower surface. The length is actually greater at the bottom than at the top by $\alpha L \Delta t$, where α is the coefficient of thermal expansion. Since the radius, R, is much greater than the thickness, h, and L much greater than $\alpha L \Delta t$, it can be easily shown from geometry that

$$R = \frac{h}{\alpha \Delta t} \tag{2}$$

and

$$c = \frac{d^2}{2R} \tag{3}$$

in which d = distance to the center of slab where curling is zero. Substituting Eq. 2 into Eq. 3 gives

$$c = \frac{\alpha \Delta t \, d^2}{2h} \tag{4}$$

Note that Δt is positive when the slab is warped up with a temperature at the top smaller than that at the bottom and negative when it is warped down.

The assumption that the slab remains in contact with the subgrade implies that the subgrade reaction always exists no matter how the slab is warped. If the slab is warped up, the subgrade will pull the slab down, and a deflection w is obtained, as shown in Figure 2. The displacement of the subgrade is thus c - w, as indicated by Eq. 1c. If w within $\{\delta'\}$ in the second term on the right side of Eq. 1a is moved to the left and combined with w on the left and c is combined with $\{F\}$, Eq. 1a becomes

$$[\overline{K}]\{\delta\} = \{\overline{F}\} \tag{5}$$

where

$[\overline{K}]$ = composite stiffness matrix of the system, and
$\{\overline{F}\}$ = composite nodal forces.

If there is no warping, then c = 0, and $\{\overline{F}\} = \{F\}$. After the displacements are obtained from Eq. 5, the stresses can also be computed.

The above derivation for upward warping also applies to downward warping. When the slab is warped down, the temperature differential is negative. If the temperature differential is the same for downward warping as for upward warping, the stresses and deflections will be the same in magnitude but opposite in sign.

Comparison With Westergaard's Solution

In the previous paper (7), the stresses and deflections due to wheel loads obtained by the finite-element method were checked with those by Westergaard's method and found to be in good agreement. To check the accuracy of the finite-element method for analyzing stresses and deflections due to temperature warping, a comparison with the Westergaard's solutions is also presented.

Westergaard (8) presented exact solutions for the stress and deflection due to warping in a concrete slab, $3\sqrt{2}\,l$ wide and infinitely long, where l is the radius of relative stiffness. His solutions for the stress and deflection along the y axis are shown by the 2 curves in Figure 3c. The stress and deflection are expressed as dimensionless ratios

in terms of σ_0 and w_0 respectively, where

$$\sigma_0 = \frac{E \alpha \Delta t}{2(1 - u)} \tag{6a}$$

$$w_0 = \frac{(1 + \mu) \alpha \Delta t l^2}{h} \tag{6b}$$

where

E = Young's modulus of concrete, and
μ = Poisson's ratio of concrete.

In the finite-element analysis, a long slab, $3\sqrt{2}$ l wide and $12\sqrt{2}$ l long as shown in Figure 3a, is employed. Because of symmetry, only a quarter of the slab is used for the finite-element analysis. The slab is divided into rectangular finite elements, as shown in Figure 3b. The input data are

$E = 3 \times 10^6$ lb/in.^{2} (21 GN/m^2),
$k = 100$ lb/in.^{3} (27.2 MN/m^3),
$h = 9$ in. (230 mm),
$\alpha = 5 \times 10^{-6}$/deg F ($9 \times 10^{-6}$/deg K), and
$\Delta t = 10$ F (5.5 K).

The positive temperature differential indicates that the slab is warped up. The radius of relative stiffness, l, is 36.95 in. (938.5 mm), which is used for determining the actual size of grid for computation.

After the stress and deflection are computed, they are expressed as dimensionless ratios and shown in Figure 3c by the small circles. The stress is considered positive when the top of the slab is in compression, which is opposite to the sign convention employed by Westergaard. The finite-element solutions check closely with Westergaard's exact solutions, thus indicating that the finite-element analysis of temperature warping as developed by the authors is theoretically correct.

ANALYSIS BASED ON PARTIAL CONTACT

The major difference in procedure between full and partial contact is that it is not necessary to consider the weight of the slab in the case of full contact, but the weight of the slab must be considered in the case of partial contact. The latter case involves 2 steps. First, the gaps and precompressions of the subgrade due to the weight of the slab or due to the weight of the slab and the warping combined are determined. These gaps and precompressions are then used to determine the stresses and deflections due to applied loads.

It should be noted that full contact is a special case of partial contact. Every problem in partial contact is analyzed first by assuming that the slab and the subgrade are in full contact. If it turns out that they are actually in full contact, no iterations are needed. If some points are found out of contact, the reactive force at those points is set to zero. The process is repeated until the same contact condition is obtained.

Partial Contact Without Initial Gaps

This case applies to new pavements not subjected to a significant amount of traffic, such as the nontraffic loop in the AASHO Road Test. Each spring in the Winkler foundation is in good condition and, if the slab is removed, will rebound to the same elevation with no initial gaps, as shown in Figure 4a. Under the weight of the slab, each spring is subjected to a precompression, as shown in Figure 4b. If the slab is warped up, gaps will form at the exterior springs, as indicated by a positive s in Figure 4c, and precompressions will form at the interior springs, as indicated by a negative s. If the slab is warped down, all springs will be under precompression, as shown in Figure 4b, except that the precompressions are not equal. The displacements due to the weight of the slab and warping combined can be determined from Eq. 1, except that the

Figure 1. Spring analogy for full contact.

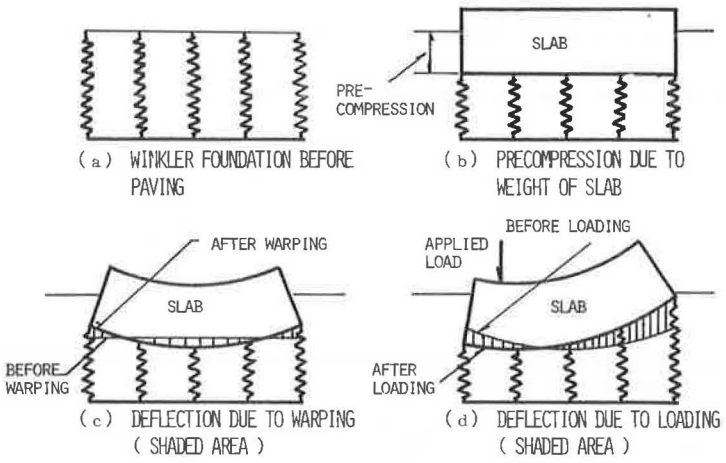

Figure 2. Warping of slab.

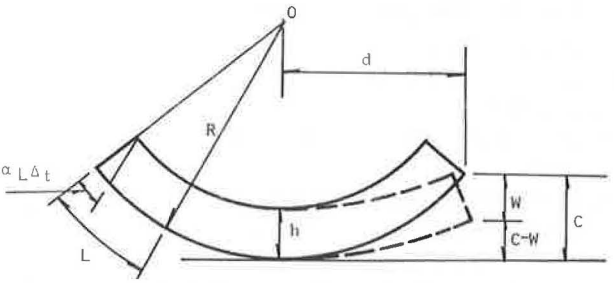

Figure 3. Comparison of finite-element solutions with Westergaard's exact solutions.

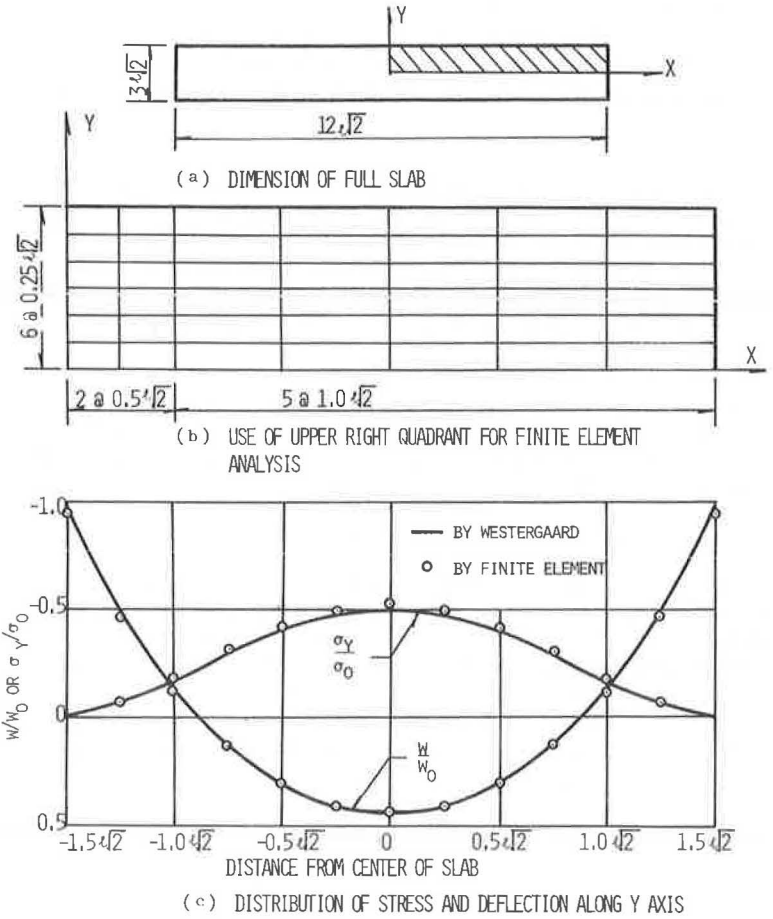

subgrade displacements are expressed as

$$\delta_i' = \begin{Bmatrix} c_i - w_i \\ 0 \\ 0 \end{Bmatrix} \qquad \text{when } w_i > c_i \tag{7a}$$

$$\delta_i' = \begin{Bmatrix} 0 \\ 0 \\ 0 \end{Bmatrix} \qquad \text{when } w_i < c_i \tag{7b}$$

Note that Eq. 7a is exactly the same as Eq. 1c for full contact and is used to start the iteration. After each iteration, a check is made on each nodal point to find whether any contact exists. If the deflection, w, is smaller than the initial curling, c, the slab is not in contact with the subgrade, and the subgrade displacement is set to zero, as indicated in Eq. 7b. Thus after each iteration, a new set of simultaneous equations is established. The process is repeated until the same equations are obtained. In most cases, this can be achieved by 5 or 6 iterations. After the deflections due to the weight and warping are determined, the gaps and precompressions can be computed and used later for computing the stresses and deflections due to the load alone.

To determine the stresses and deflections due to the load alone requires that the gaps and precompressions shown in Figures 4b or 4c, depending on whether warping exists, first be determined. When these gaps and precompressions are used as s, the deflections due to the load alone, as shown in Figure 4d, can be determined from Eq. 1, except that the subgrade displacements are expressed as

$$\delta_i' = \begin{Bmatrix} 0 \\ 0 \\ 0 \end{Bmatrix} \qquad \text{when } w_i < s_i \tag{8a}$$

$$\delta_i' = \begin{Bmatrix} s_i - w_i \\ 0 \\ 0 \end{Bmatrix} \qquad \text{when } w_i > s_i \text{ and } s_i > 0 \tag{8b}$$

$$\delta_i' = \begin{Bmatrix} -w_i \\ 0 \\ 0 \end{Bmatrix} \qquad \text{when } w_i > s_i \text{ and } s_i < 0 \tag{8c}$$

When w is checked with s, downward deflection is considered positive, upward deflection is considered negative, gap is considered positive, and precompression is considered negative. First, assume that the slab and the subgrade are in full contact and the deflections of the slab due to the applied load are determined. Then check the deflections with s and form a new set of equations based on Eq. 8. The process is repeated until the same equations are obtained.

When the slab and the subgrade are in partial contact, the principle of superposition no longer applies. To determine the stresses and deflections due to an applied load requires that the deformed shape of the slab immediately before the application of the load be computed first. Since the deformed shape depends strongly on the condition of warping, the stresses and deflections due to loading are affected appreciably by warping. This fact was borne out in both the Maryland (9) and the AASHO (10) road tests.

In the method presented here, the stresses and deflections due to weight and warping are computed separately from those due to loading. This is desirable because the modulus of subgrade reaction under the sustained action of weight and warping is much smaller than that under the transient load of traffic. If the same modulus of subgrade

reaction is used, the stresses and deflections due to the combined effect of weight, warping, and loading can be computed in the same way as those due to weight and warping, except that additional nodal forces are needed to account for the applied loads.

Partial Contact With Initial Gaps

This case applies to pavements subjected to a high intensity of traffic, such as the traffic loops in the AASHO Road Test. Because of pumping or plastic deformation of the subgrade, some springs in the Winkler foundation become defective and, if the slab is removed, will not return to the original elevation. Thus, initial gaps are formed, as indicated by the 2 exterior springs shown in Figure 5a. These gaps, s, must be assumed before an analysis can be made.

The displacements due to the weight of slab, as shown in Figure 5b, can be determined from Eq. 1, except that the subgrade displacements must be expressed as

$$\delta_i' = \begin{Bmatrix} s_i - w_i \\ 0 \\ 0 \end{Bmatrix} \qquad \text{when } w_i > s_i \tag{9a}$$

$$\delta_i' = \begin{Bmatrix} 0 \\ 0 \\ 0 \end{Bmatrix} \qquad \text{when } w_i < s_i \tag{9b}$$

First, assume that the slab and the subgrade are in full contact. The vertical deflections of the slab are determined from Eq. 1. Then check the deflection at each node against the gap, s. If the deflection is smaller than the gap, as shown by the left spring in Figure 5b, Eq. 9b is used. If the deflection is greater than the gap, as shown by the other springs in Figure 5b, Eq. 9a is used. The process is repeated until the same equations are obtained. After the deflections are obtained, the gaps and precompressions can be computed and used later for computing the stresses and deflections due to loading, if no warping exists.

If the springs are of the same length, as shown in Figure 1, the weight of the slab will result in a uniform precompression, and no stresses will be set up in the slab. However, if the springs are of unequal lengths, the deflections will no longer be uniform, and stressing of the slab will occur.

Figure 5c shows the combined effect of weight and warping when the slab is warped down. The reason that downward warping is considered here, instead of the upward warping, is that the case of upward warping is similar to that shown in Figure 4c except that the gaps are measured from the top of the defective springs. Because the method is applicable to both upward and downward warping, the case of downward warping is used for illustration. The procedure for determining the deflections is similar to that involving the weight of slab alone except that the initial curling of the slab, as indicated by Eq. 4, is added to the gap shown in Figure 5a to form the total gap and precompression, s, for use in Eq. 9. Since the gap is either positive or zero and the initial curling may be positive or negative, depending on whether the slab is warped up or down, s may be positive or negative. After the deflections of the slab are obtained, the gaps and precompressions, as shown in Figure 5c, can be determined. These gaps and precompressions are used for computing the stresses and deflections due to the load alone, as shown in Figure 5d.

The above method was programmed for an IBM 360 computer, model 65, available at the University of Kentucky. The program can determine the stresses and deflections due to the weight of slab, the weight of slab plus warping, or the applied wheel loads in concrete pavements consisting of 1 slab, 2 slabs connected by a transverse joint, or 4 slabs connected by a longitudinal and a transverse joint. The efficiency of load transfer at each joint can be specified, and the same general principle, as described in the previous paper (7), is used in treating the doweled joints. To save the computer stor-

age, load transfer is evaluated by an iterative procedure so that each slab is considered separately instead of all at the same time.

COMPARISON WITH AASHO ROAD TEST

In the previous paper (7), the edge stress under moving wheel loads and the stress distribution under vibratory loads, as measured in the AASHO Road Test, were compared with the finite-element solutions based on full subgrade contact. It was found that the finite-element method checked reasonably well with the experimental measurements if a k value of 300 lb/in.^{3} (81.5 MN/m^3) was used for moving loads and 900 lb/in.^{3} (244 MN/m^3) for vibratory loads. The agreement between the observed and the computed stresses based on full contact is not surprising because, unless the load is applied close to the corner of the slab, the condition of contact does not have a large effect on stresses. In view of the fact that the corner deflections are affected more significantly by the condition of contact, the corner deflections observed in the AASHO Road Test will also be presented and compared with the finite-element solutions.

Warping of Slabs Due to Temperature Differential

In the AASHO Road Test, the vertical movement of slabs due to the daily variation of temperature was measured on the nontraffic loop, and typical contours of vertical movement were published by the Highway Research Board (10). It is interesting to compare these measurements with finite-element solutions.

In the finite-element analysis for temperature warping, the following material properties are used: $E = 5.25 \times 10^6$ lb/in.^{2} (36.2 GN/m^2), $\mu = 0.28$, and k = 50 lb/in.^{3} (13.6 MN/m^3). The Young's modulus is the static modulus measured at the road test, which is smaller than the 6.25×10^6 lb/in.^{2} (43.1 GN/m^2) reported for the dynamic modulus. Although the k value obtained by the plate-bearing test at the road test varies from 63 to 135 lb/in.^{3} (17.1 to 36.7 MN/m^3), a smaller value is used here because the pressure applied to the subgrade due to temperature warping generally lasts for several hours instead of the 15 s used for the plate-bearing test.

In the AASHO Road Test, the temperature was measured in a 6.5-in. (165-mm) slab. The temperature at a point ¼ in. (6 mm) below the top surface of the 6.5-in. (165-mm) slab minus the temperature at a point ½ in. (13 mm) above the bottom surface was referred to as the standard temperature differential. The maximum standard temperature differential for the month of June and July, in which most of the warping measurements were made, averaged about -8.8 F (-4.9 K) when the slab is warped up and 18.5 F (10.3 K) when it is warped down. In line with the finite-element formulation, the sign convention for temperature differential used in this paper is opposite to that in the AASHO Road Test. A positive temperature differential always indicates that the temperature is smaller at the top than at the bottom. This convention applies hereafter whenever the standard temperature differential is referred to. Based on the finding of the Arlington test (2), there is a straight-line gradient in temperature between the upper and lower surfaces in the early morning and in the afternoon when the maximum temperature differentials occur. Therefore, the maximum temperature differential for a 6.5-in. (165-mm) slab at the road test should be 10 F (5.5 K) when the slab is warped up and -21 F (11.7 K) when it is warped down. Although temperatures in other thicknesses of slab were also measured in the AASHO Road Test, the data published by the Highway Research Board (10) are not detailed enough for use in an analysis. However, the published data do show that the temperature differential is not proportional to the thickness of the slab and that the increase in temperature differential is not so rapid as the increase in thickness. Based on the result of the Arlington test (2) that the maximum temperature differential of a 9-in. (230-mm) slab is 1.27 times greater than that of a 6-in. (150-mm) slab, the temperature differentials for 5-in. (130-mm), 9.5-in. (240-mm), and 12.5-in. (320-mm) slabs are calculated and given in Table 1. Only these 3 thicknesses are considered in this study because the stresses due to vibratory loads were measured on slabs of these thicknesses.

In the finite-element analysis of warping and loading, a 2-slab system rather than a 4-slab system is employed because a comparison between the 2 systems shows that the

Figure 4. Partial contact without initial gaps.

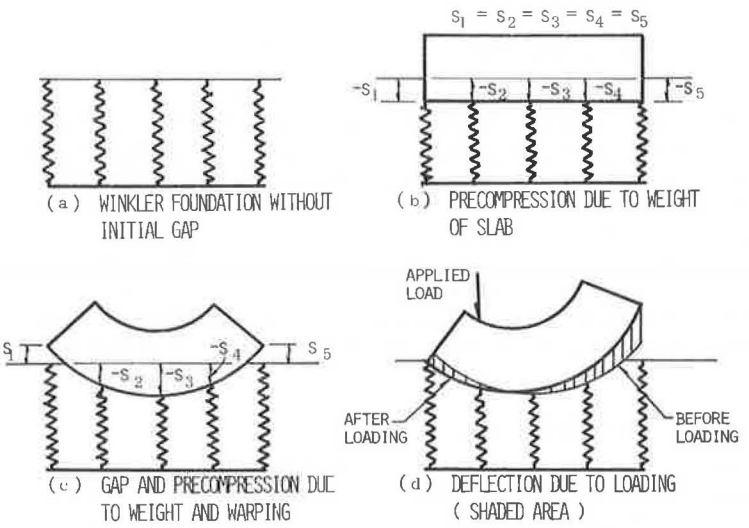

Figure 5. Partial contact with initial gaps.

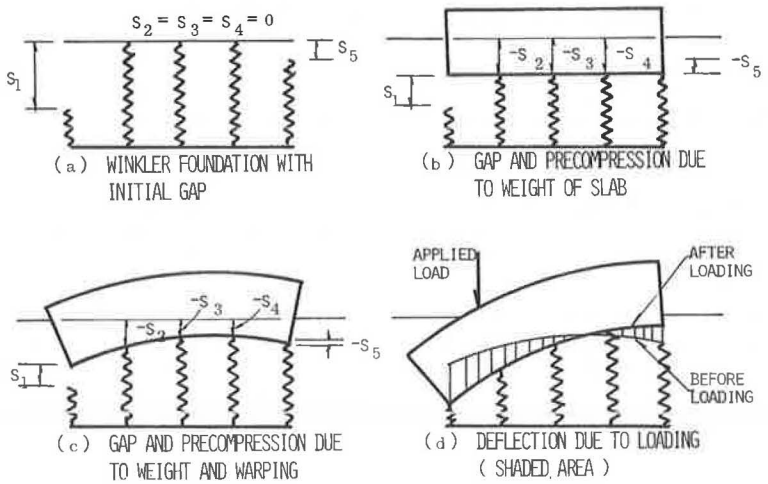

Table 1. Temperature differentials for analyzing AASHO Road Test rigid pavements.

Thickness (in.)	Warp Up (deg F)	Warp Down (deg F)
5	8.7	-18.3
9.5	12.7	-26.2
12.5	15.4	-31.4

Note: 1 in. = 25.4 mm; (deg F + 459.67)/1.8 = deg K.

2 slabs on the other side of the longitudinal joint have very little effect on the stresses and deflections at the corner region where measurements were made. The slabs are divided into finite elements with part of the nodal numbers and the 4 loading positions shown in Figure 6. Because of symmetry, only one slab is theoretically needed for the analysis of warping. However, 2 slabs are employed because the gaps and precompressions due to the weight of the slab and warping will be used for computing the stresses due to loading. As the experimental measurements were made on the nontraffic loop, the case of partial contact without initial gaps is assumed. The vertical movements are obtained in 3 steps. First, determine the gaps and precompressions due to the weight of the slab and the upward warping, as shown in Figure 4c. Then, determine the gaps and precompressions due to the weight of the slab and the downward warping. Finally, obtain the vertical movements by subtracting the former from the latter.

Figure 7 gives a comparison of the vertical movements measured at the road test with those computed by the finite-element method. The solid lines are the finite-element solutions based on full contact, the crosses are those based on partial contact, and the small circles are the experimental measurements obtained from the typical contours published by the Highway Research Board (10). Starting from left to right, the figure shows the vertical movements along the pavement edge, the diagonal of a corner, and the transverse joint. The numerals along the abscissa refer to the nodal number shown in Figure 6.

Under the temperature differentials assumed, most parts of the slabs, except that at the extreme corner, remain in contact with the subgrade, so there is very little difference between full and partial contact. The theoretical movements are somewhat smaller than the observed movements, but the general trends are similar. In view of the fact that the assumed temperature differentials may not be the same as those when measurements were made and that the actual k value may be different from the 50 lb/in.^{3} (13.6 MN/m^3) assumed, the agreement between the theoretical solutions and the experimental measurements should be considered satisfactory.

The results of the 9.5-in. (240-mm) slab is left out purposely because the experimental measurements were inconsistent. The experimental data show that the movements of the 9.5-in. (240-mm) slab are generally greater than those of the 5-in. (130-mm) and 12.5-in. (320-mm) slabs in the 15-ft (4.6-m) nonreinforced sections but smaller in the 40-ft (12.2-m) reinforced sections. This fact was pointed out in the AASHO report (10), but no explanation could be made. The theoretical solutions based on a 15-ft (4.6-m) panel check well with the experimental measurements on the 40-ft (12.2-m) panel, but not so good with those on the 15-ft (4.6-m) panel.

Stress Distribution Under Vibratory Loads

In the previous paper (7), a comparison of stresses under vibratory loads was made between the finite-element solutions based on full contact and the experimental measurements. It was found that, when $E = 6.25 \times 10^6$ lb/in.^{2} (43.1 GN/m^2), $\mu = 0.28$, and k = 900 lb/in.^{3} (244 MN/m^3), the finite-element solutions checked quite well with the experimental measurements, except for the minor principal stress in the 5-in. (130-mm) and 9.5-in. (240-mm) slabs. It was indicated that these discrepancies were due to the warping of slabs because the experimental data were taken during the early morning hours when the corners and edges of the slab were warped upward and part of the slab was not in contact with the subgrade. With the capability of evaluating the effect of warping on loading, as developed in this study, it will be interesting to find the effect of upward warping on the theoretical stresses. Because the stresses were measured on the nontraffic loop, the case of partial contact without initial gaps is assumed. The gaps and precompressions due to the weight of slab and the upward warping, as shown in Figure 4c and obtained in the previous section, are used for computing the stresses due to the applied load.

Figure 8 shows a comparison of the theoretical and experimental distribution of major and minor principal stresses. The figure is the same as that presented in the previous paper (7), except that the results based on partial contact are included. Four loading

Figure 6. Loading positions and finite-element grid.

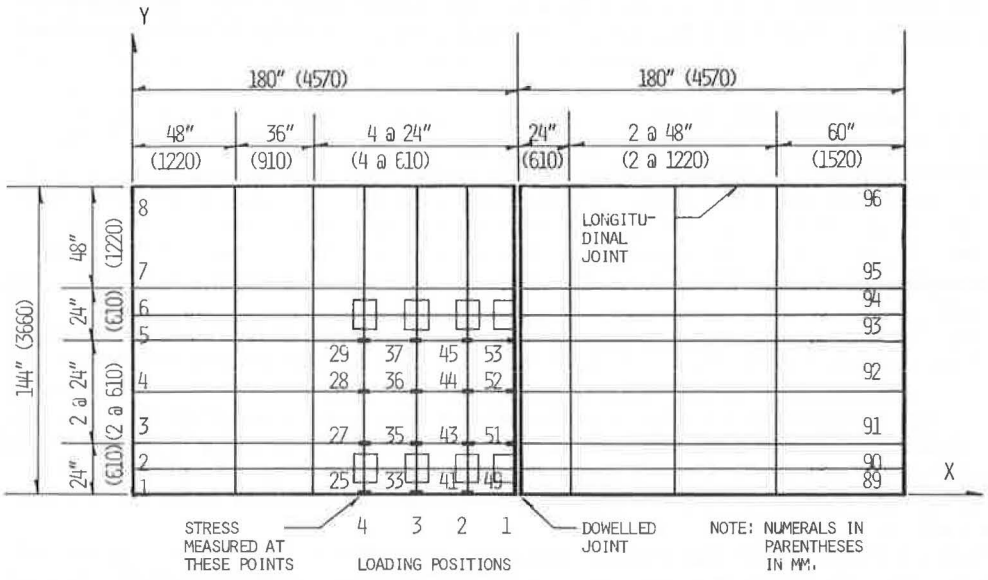

Figure 7. Comparison of theoretical and observed vertical movements due to warping.

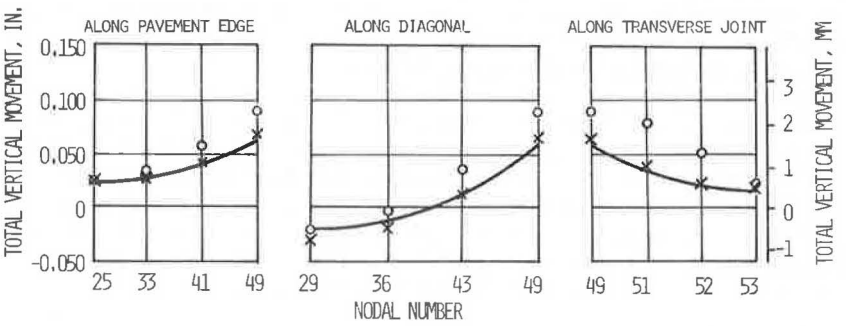

(a) 5 INCH SLAB (130 MM)

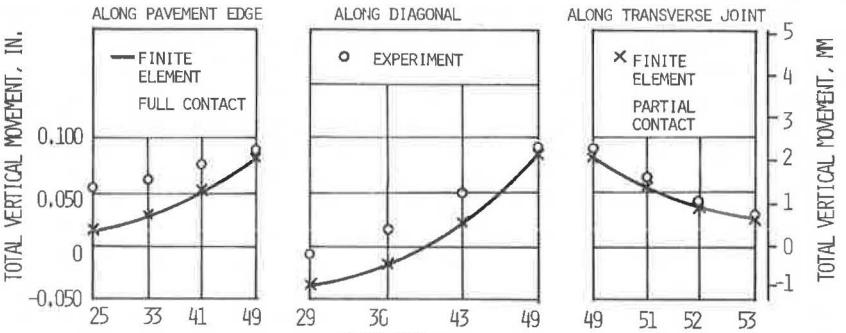

(b) 12.5 INCH SLAB (320 MM)

positions, as shown in Figure 6, are considered. For loading position 1, the stresses are those along the joint. For other loading positions, they are along a line connecting the centers of the 2 pads. The figure shows that a better agreement between the theoretical solutions and the experimental measurements is obtained if the effect of warping is considered. The significant improvement in the minor principal stresses for the 5-in. (130-mm) slab is attributed to the fact that warping causes a loss of contact over a large area near the corner of the slabs. The effect of warping is quite small for the 12.5-in. (320-mm) slab because only a small area near the corner is not in contact. The figure also shows that upward warping has a large effect on the minor principal stresses when the load is applied near the corner, as indicated by loading position 1, but very little effect on both the major and minor principal stresses when the load is far from the corner.

Corner Deflections in Pavements on Traffic Loops

All previous comparisons between the finite-element solutions and the experimental measurements are made on the nontraffic loop, and the solutions are based on partial contact withoug initial gaps. To demonstrate the applicability of the method to actual pavements with initial gaps, we compute by the finite-element method the corner deflections at the traffic loops due to an 18-kip (80-kN) single-axle load and compared them with the rebound deflections measured by a Benkelman beam. The following material properties were used in the analysis: $E = 6.25 \times 10^6$ lb/in.^{2} (43.1 GN/m^2), $\mu = 0.28$, and $k = 300$ lb/in.^{3} (81.5 MN/m^3). These values are the same as those used in the previous paper (7) for analyzing the dynamic edge stress and are based on the transient nature of the rebound measurements.

The 2-slab system is divided into finite elements, as shown in Figure 9. The tire imprints are converted into 4 rectangular areas, each 9.93 in. (252.2 mm) by 6.83 in. (173.5 mm). The spacing between is 11.5 in. (292.1 mm). The thickness of slabs is assumed to be 6.5 in. (165 mm). Three temperature differentials, i.e., 10, 0, and -21 F (5.5, 0, and -11.7K), are employed, which correspond to standard temperature differentials of 8.8, 0, and -18.5 F (4.9, 0, and -10.3 K) respectively. The standard temperature differential is the difference in temperature between 2 points in a 6.5-in. (165-mm) slab, one ¼ in. (6 mm) below the top and the other ½ in. (13 mm) above the bottom.

Figure 10 shows a comparison of the finite-element solutions and the experimental measurements. The smooth curve, which represents the relation between corner deflections and standard temperature differentials, is obtained from an empirical equation developed from the AASHO Road Test (10) for a slab of 6.5 in. (165 mm). In both the case without initial gaps and the case with initial gaps, the gaps and precompressions due to the weight of the slab and the warping, if the latter exists, are determined first and then used for computing the stresses and deflections due to the axle load. The average computer time is 40 s for analyzing the weight and warping for each temperature differential and 35 s for analyzing the axle load.

Figure 10 shows that the finite-element solutions based on partial contact without initial gaps do not check with the experimental measurements. If no initial gaps exist between the slab and the subgrade, the corner deflections due to the applied load are nearly the same no matter whether the slab is flat with a 0 temperature differential or is warped down with a negative temperature differential because full contact prevails in both cases. However, if gaps are assumed to exist along the edges and joints, the results, as indicated by the crosses, are much improved and check closely with the experimental measurements. The fact that the gaps have practically no effect on corner deflections at a standard temperature differential of -18.5 F (-10.3 K) is that at this temperature differential the gaps are not large enough to cause a loss of subgrade contact at the corner. If larger gaps are provided so that the corner of the slab is not in contact with the subgrade, the corner deflection will certainly increase.

The initial gaps assumed in the analysis are 0.04 in. (1mm) along the edge and 0.02 in. (0.5 mm) along the joint. These gaps are the results of pumping and plastic deformation of the subgrade and should be greater at the edge than at the joint because under a

Figure 8. Comparison of theoretical and experimental distribution of major and minor principal stresses.

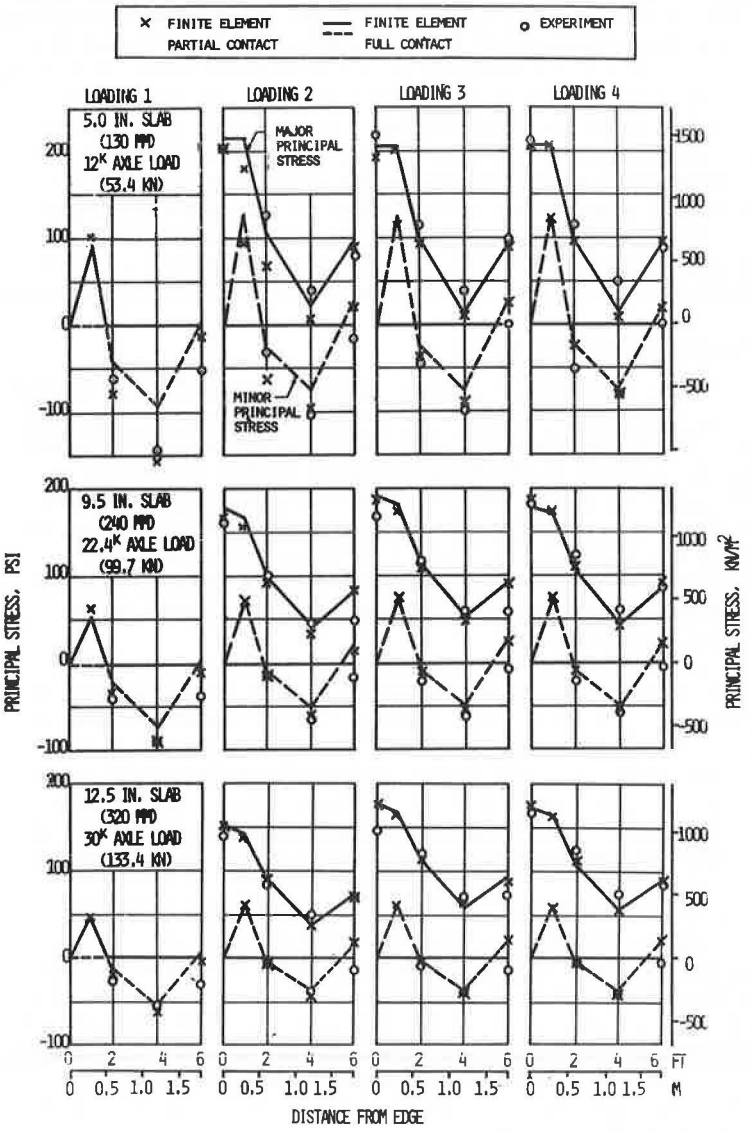

Figure 9. Finite-element network and location of 18-kip single-axle load.

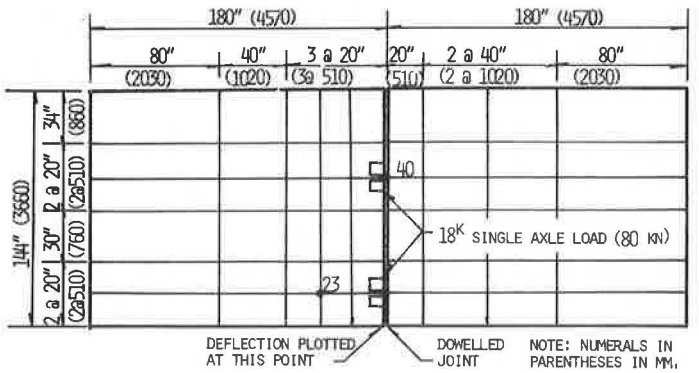

Figure 10. Corner deflections due to 18-kip single-axle load.

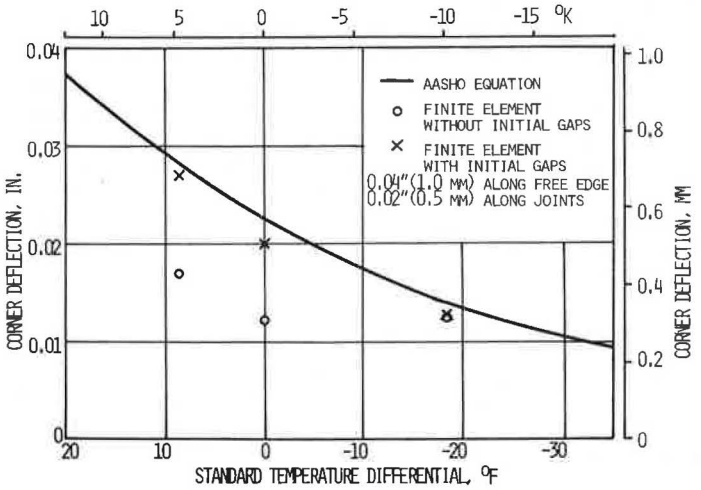

given wheel load the deflection is greater at the edge than that at the joint. Although the use of the above gaps yields results comparable to the experimental measurements, it is possible that for other pavements, in addition to the edge and joint, initial gaps also exist at other points near the edge and joint. The amount and distribution of these initial gaps depend on a variety of factors, such as type of subgrade, magnitude and repetitions of wheel loads, thickness of slab, and climatic conditions. Further research is needed to ascertain the amount and distribution of these gaps so that they can be used directly for determining the stresses in concrete pavements.

SUMMARY AND CONCLUSIONS

A finite-element method programmed for a high-speed computer was developed for analyzing concrete pavements with partial subgrade contact. The partial contact may result from the pumping and plastic deformation of the subgrade in combination with the upward warping of the slab. The lack of a theoretical method for analyzing this practical problem has plagued highway engineers for several decades. It is believed that the method presented here provides an efficient tool for solving this complex problem.

The method presented is based on the classical theory of thin plates on Winkler foundation. The accuracy of the method for computing temperature stresses is verified by assuming that the slab and the subgrade are in full contact and by making comparisons with Westergaard's exact solutions. The validity of the method in predicting the stresses and deflections in actual pavements is indicated by comparisons with the experimental measurements from the AASHO Road Test. The method has potential application in the design of rigid pavements.

Based on the condition of contact, the analysis of rigid pavements is divided into 3 cases: full contact, partial contact without initial gaps, and partial contact with initial gaps. In the case of full contact, the stresses and deflections due to wheel loads can be computed directly, disregarding the weight and warping of slabs; in the 2 cases of partial contact, the deformed shape of the slabs due to the combined effect of weight and warping must first be determined and then used for computing the stresses and deflections due to wheel loads. A comparison between the finite-element solutions and the experimental measurements made on the nontraffic loop at the AASHO Road Test clearly indicates that, if no initial gaps exist between the slab and the subgrade, the assumption of full contact generally yields reasonable results, even if the slab is warped up. However, in some cases the agreement is improved when partial contact is assumed. If there are initial gaps between the slab and the subgrade as a result of pumping and

plastic deformation, the assumption of full contact is no longer valid, and the method based on partial contact with initial gaps should be employed.

A major contribution of this paper is the development of a method that takes into consideration the effect of warping on the stresses and deflections due to wheel loads. The application of the method based on partial contact without initial gaps is straightforward. Compared with the method based on full contact, it requires very little additional information other than the temperature differential between the top and bottom of the slabs. However, the applications of the method based on partial contact with initial gaps is more difficult because it requires a prior knowledge of the amount of gaps at various points beneath the slabs. These gaps are larger near the pavement edges and joints and become negligible in the interior of slabs. They must be properly estimated before an analysis can be made.

ACKNOWLEDGMENTS

The study reported here is part of a faculty research program sponsored by the Department of Civil Engineering, University of Kentucky, and the University of Kentucky Research Foundation. The support given by the University of Kentucky Computing Center for the use of the computer is appreciated.

REFERENCES

1. Westergaard, H. M. Stresses in Concrete Pavements Computed by Theoretical Analysis. Public Roads, Vol. 7, 1926, pp. 25-35.
2. Teller, L. W., and Sutherland, E. C. The Structural Design of Concrete Pavements. Public Roads, Vol. 16, 1935, pp. 145-158, 169-197, 201-221; Vol. 17, 1936, pp. 143-171, 175-192; Vol. 23, 1942, pp. 167-211.
3. Bradbury, R. D. Reinforced Concrete Pavements. Wire Reinforcement Institute, Washington, D.C., 1938.
4. Kelley, E. F. Application of the Results of Research to the Structural Design of Concrete Pavement. Public Roads, Vol. 20, 1939, pp. 83-104.
5. Spangler, M. G. Stresses in the Corner Region of Concrete Pavements. Eng. Exp. Station, Iowa State College, Ames, Bull. 157, 1942.
6. Pickett, G. Concrete Pavement Design: Appendix III—A Study of Stresses in the Corner Region of Concrete Pavement Slabs Under Large Corner Loads. Portland Cement Association, 1951, pp. 77-87.
7. Huang, Y. H., and Wang, S. T. Finite-Element Analysis of Concrete Slabs and Its Implications on Rigid Pavement Design. Highway Research Record 466, pp. 55-79, 1973.
8. Westergaard, H. M. Analysis of Stresses in Concrete Pavement Due to Variations of Temperature. HRB Proc., Vol. 6, 1926, pp. 201-215.
9. Road Test One-MD, Final Report: Effect of Controlled Axle Loadings on Concrete Pavement. HRB Spec. Rept. 4, 1952.
10. The AASHO Road Test: Report 5—Pavement Research. HRB Spec. Rept. 61E, 1962.